Eur. Phys. J. C (2025) 85:844
https://doi.org/10.1140/epjc/s10052-025-14596-x

THE EUROPEAN PHYSICAL JOURNAL C

Regular Article - Theoretical Physics

Comprehensive analysis of dark energy stars in R-squared gravity

Ayan Banerjee[1,a], **Safiqul Islam**[2,3,b], **Javlon Rayimbaev**[4,5,6,7,c], **Inomjon Ibragimov**[8,d], **Sokhibjan Muminov**[9,e], **Ikram Davletov**[10,f]

[1] Astrophysics and Cosmology Research Unit, School of Mathematics, Statistics and Computer Science, University of KwaZulu–Natal, Private Bag X54001, 4000 Durban, South Africa
[2] Department of Basic Sciences, General Administration of Preparatory Year, King Faisal University, P.O. Box 400, 31982 Al Ahsa, Saudi Arabia
[3] Department of Mathematics and Statistics, College of Science, King Faisal University, P.O. Box 400, 31982 Al Ahsa, Saudi Arabia
[4] National University of Uzbekistan, 100174 Tashkent, Uzbekistan
[5] Tashkent International University of Education, Imom Bukhoriy 6, 100207 Tashkent, Uzbekistan
[6] University of Tashkent for Applied Sciences, Str. Gavhar 1, 100149 Tashkent, Uzbekistan
[7] Tashkent State Technical University, 100095 Tashkent, Uzbekistan
[8] Kimyo International University in Tashkent, Shota Rustaveli Street 156, 100121 Tashkent, Uzbekistan
[9] Mamun University, Bolkhovuz Street 2, 220900 Khiva, Uzbekistan
[10] Department of Technique, Urgench State University, Kh. Alimjan Str. 14, 221100 Urgench, Uzbekistan

Received: 10 May 2025 / Accepted: 28 July 2025

Abstract This study examines the structure and stability of dark energy stars within the context of R^2 gravity, with the gravity model defined by $f(R) = R + aR^2$ (the Starobinsky model). Specifically, dark energy is a mysterious force that can prevent the gravitational collapse of compact objects to singularities. To characterize dark energy, we consider modified Chaplygin fluid as an equation of state (EoS) of matter and study its mass-radius relation for different model parameters. By numerically solving the modified Tolman–Oppenheimer–Volkoff (TOV) equations, our primary objective is to examine the influence of variations in the R^2 gravity parameter a on the energy density, pressure, mass-radius and mass-central density relationships of dark energy stars. Our findings reveal that the variation of a does not significantly impact on the $(M - R)$ relations but comfortably exceeds the $2M_{\odot}$ limit. Additionally, we examine the dynamical stability of these stars by evaluating the static stability criterion, adiabatic index, and sound speed. Finally, we compare our results with various astrophysical observational data and discuss future observations that could validate the predictions of our model.

[a] e-mail: ayanbanerjeemath@gmail.com
[b] e-mail: sislam@kfu.edu.sa
[c] e-mail: javlon@astrin.uz (corresponding author)
[d] e-mail: i.ibragimov@kiut.uz
[e] e-mail: madaminov_bekzod@mamunedu.uz
[f] e-mail: ikram.d@urdu.uz

1 Introduction

Dark energy stars have been proposed as a hypothetical alternative to classical black holes. In these models, gravitational collapse does not culminate in the formation of a singularity characterized by infinite density, nor does it create an event horizon. Instead, quantum effects-specifically those associated with vacuum energy density or dark energy -intervene to arrest the collapse, yielding a stable, compact object. This concept was first developed by George Chapline in the early years of the twentieth century [1,2]. He suggested that dark energy stars resolve paradoxes, such as the black hole information loss problem. Mazur and Mottola [3] proposed gravastars as a new class of astrophysical objects, with an internal de Sitter core surrounded by a thin shell. They observed gravastars as stable and non-singular alternatives to black holes. Yazadjiev et al. [4] studied non-perturbative and self-consistent rotating neutron stars within the framework of R^2 gravity. A key finding in this context is the impact of stellar rotation on properties such as mass-radius relations and moment of inertia. Moreover, the effects predicted by this gravity is significantly different from standard GR. Since the discovery of the accelerated expansion of the universe, it is of utmost importance to introduce dark energy as a key component of the matter distribution. This growing interest in fluids, particularly in the contexts of gravitational collapse and star formation, demands a careful study of the energy conditions

Published online: 05 August 2025

and the specific roles played by the pressure components, as investigated by Chan et al. [5].

Any physically realistic astrophysical object must exhibit stability to persist in the universe. If dark energy stars are unstable, they would rapidly tend to collapse or evolve into another configuration, such as a black hole, rendering them unsustainable as alternatives. Lobo [6] developed exact solutions for compact objects characterized by dark energy interiors, demonstrating that these configurations can maintain stability when subjected to any radial perturbations. Interestingly, this model also elucidates the potential for smooth transitions between regions of normal and exotic matter within stars. In this regard, a dark energy star may be considered a compact star, if it exists; however, it remains a theoretical concept now. Numerous studies have explored different possibilities regarding their internal matter, including normal nuclear matter, quarks, hyperons, Bose–Einstein condensates, dark matter, and dark energy. Recently, compact objects composed of such elusive dark energy have drawn much interest [5–19]. The comprehensive review of Berti et al. [20] demonstrates how gravitational wave and electromagnetic observations can be used to test GR and recognize deviations that point toward exotic alternatives, such as dark energy stars or gravastars. It also outlines the challenges along with the prospects associated with detecting such objects. Further studies by Bueno et al. [21] reveal how perturbations around exotic compact objects, such as Kerr-like wormholes associated with dark energy interiors, can produce echo signatures in gravitational wave observations. The authors propose that such echoes could provide observational evidence distinguishing these objects from classical black holes. Dark energy models include quintessence, K-essence, tachyon, phantom, dilatonic fields, cosmological constant, and Chaplygin gas. Detailed reviews are available in Refs. [22,23]. However, Einstein's theory of general relativity (GR) is not the only possible theory of gravity. Numerous modified gravity theories (MGTs) extending GR have been proposed to explain the cosmic acceleration. In this context, some studies have been done for finding the compact astrophysical objects in MGTs [24–30]. For example, within $f(R, G)$ gravity, authors have explored the possibility of existence for a compact star composed of anisotropic dark energy and isotropic normal matter. This investigation provides valuable insights into the behavior of dark energy stars, also addressing the validity of MGTs. Further, the innovative work of Mak et al. [31], provided a general solution to the EFEs, where static, spherically symmetric fluid spheres while considering pressure isotropy. The authors reformulated the pressure isotropy as a Riccati-type differential equation and obtained regular, exact solutions. Both isotropic and anisotropic dark energy stars within the framework of rainbow gravity have been explored in [32]. The authors derived a modified hydrostatic equilibrium equation, expressed by the extended Chaplygin equation of state, and subsequently solved this equation for both scenarios. Pretel et al. [17] studied dark energy stars with Chaplygin-type EoS, and further analyzed both isotropic and anisotropic pressure configurations within the framework of GR. The research demonstrated stability under radial perturbations and assessed key physical properties, including tidal deformability and moment of inertia. Kumar et al. [33], developed a novel solution for a spherically symmetric spacetime by exploring the Chaplygin gas as an EoS. To obtain the solution, the Tolman metric potential proposed by Tolman [34] is employed to solve the Einstein field equations. The resulting model exhibits well-behaved physical characteristics and satisfies all the energy conditions.

Borowiec et al. [35] explored Palatini R^2 gravity with generalized Chaplygin gas EoS, which explains both the present accelerated expansion and early endogenous inflation, triggered by a type III freeze singularity. The study in [36] involves various $f(R)$ gravity models associated with different EoSs, which include the standard, generalized, and modified Chaplygin gas, and offers insights into their integration within the $f(R)$ framework. In addition, the polytropic and Chaplygin $f(R)$ gravity models in de Sitter spacetime satisfy the inflation conditions. In Ref. [37], the authors investigate the formation of compact stars within the framework of modified $f(R)$ gravity, particularly the Starobinsky model, $f(R) = R + aR^2$. Although it does not include the Chaplygin gas EoS directly, it lays the foundation for exploring how such an EoS could interact with R^2 gravity in stellar structures. Errehymy et al. [38] applied the TOV equations to a Chaplygin-type fluid to investigate the behavior of astrophysical configurations. They examined the phantom regime, where the pressure magnitude exceeds the energy density, resulting in truncated spheroidal geometries, and the normal regime, corresponding to 3D spheroidal geometries. More research shows how the Chaplygin gas EoS can be incorporated into R^2 gravity model, including the Starobinsky model, to demonstrate the various astrophysical and cosmological phenomena (see e.g., Refs. [39–43]).

This study is motivated by the desire for singularity-free alternatives to classical black holes in modified gravity that circumvent gravitational collapse singularities predicted by GR, which are likely to be avoided if dark energy and quantum gravity effects are taken into account. In this context, we consider higher-order curvature corrections to GR in terms of the Starobinsky model with the Lagrangian ($f(R) = R + aR^2$) because it is theoretically viable and plays an important role in early-universe inflationary dynamics. At the same time, since the modified Chaplygin gas EoS interpolates between dark matter and dark energy behaviors and satisfies theoretical viability conditions, we use this EoS to model the interior matter content of compact objects. Given that recent astrophysical observations, such

as gravitational wave events and precise pulsar timing measurements, favor ultra-compact stellar remnants with masses larger than $(2M_\odot)$, here we study whether dark energy stars in the Starobinsky model of $f(R)$ gravity can be realized as physically viable, stable objects obeying observational bounds. This framework, which combines modified gravity with exotic matter content, forms the basis for our detailed analysis.

In this study, we examine a spherically symmetric configuration under the assumption of isotropic pressure. Although it is acknowledged that compact stellar objects with extremely high central densities may inherently exhibit pressure anisotropies, particularly due to microphysical processes such as phase transitions, strong magnetic fields, or superfluidity, our aim here is to provide a foundational analysis of dark energy stars within the framework of Starobinsky gravity. The adoption of an isotropic pressure model facilitates a clearer interpretation of the gravitational modifications introduced by the R^2 term without additional model-dependent assumptions related to anisotropy. The rest of this paper is organized as follows: In Sect. 2, we present a concise review of Starobinsky gravity and derive the modified TOV equations for non-rotating stars. In Sect. 3, we present EoS concerning the modified Chaplygin gas as an exotic fluid for dark energy star structure. Section 4 is dedicated to the numerical solution of the modified TOV equation, where we present a complete analysis of dark energy stars. The stability analysis has been incorporated in 5. In Sect. 6, we summarize our findings and provide concluding remarks.

Notations and conventions: We assume Newton's universal gravitational constant G and the velocity of light in a vacuum c to be $G = c = 1$. Additionally, we utilize the metric convention $g_{\mu\nu} = \text{diag}(-1, 1, 1, 1)$. Here, $\text{M}_\odot$ represents the mass of the Sun.

2 Field equations and set up

The $f(R)$ gravity is a notable example for modified gravity theory. In this approach, the Lagrangian is replaced by the Ricci scalar with a function $f(R)$, resulting in an action described by

$$S = \frac{1}{16\pi}\int d^4x\sqrt{-g}\,f(R) + S_{\text{matter}}(\psi_i, g_{\mu\nu}), \tag{1}$$

where $f(R)$ is a function only of the Ricci scalar R. In the second segment of the action, S_{matter} denotes the action of the matter field depending on the metric tensor and the matter field ψ_i. To avoid pathological phenomena such as tachyonic instabilities and ghosts, the viable $f(R)$ theories must comply with the following conditions as stipulated in references [29,44]

$$\frac{d^2f}{dR^2} \geq 0, \quad \frac{df}{dR} > 0, \tag{2}$$

respectively. In this study, we consider the Starobinsky gravity model, and the functional form of $f(R)$ is specified as $f(R) = R + aR^2$, where the parameter a is assumed to satisfy $a \geq 0$, supporting the inequalities specified in Eq. (2) [45]. The model's key parameter a has dimensions of $[mass]^{-2}$, and it can be expressed as $a = 1/M^2$, thereby indicating that the mass scale M now serves as the theory's free parameter. Moreover, the choice of $a = 0$ allows us to recover the GR solution again.

On the one hand, solving fourth-order differential equations within $4D$ spacetime often poses considerable difficulties. By this reason, it is more comfortable to adopt a conformal transformation by introducing the new scalar field φ and the new metric $\tilde{g}_{\mu\nu}$ [30,46,47], which yields

$$\tilde{g}_{\mu\nu} = pg_{\mu\nu} = A^{-2}(\varphi)g_{\mu\nu}, \tag{3}$$

where $A(\varphi = \exp(-\phi/\sqrt{3})$. Employing this transformation leads us to rewrite the action (1) in the Einstein frame as

$$S = \frac{1}{16\pi G}\int d^4x\sqrt{-\tilde{g}}[\tilde{R} - 2\tilde{g}^{\mu\nu}\partial_\mu\varphi\partial_\nu\varphi - V(\varphi)] + S_M[\psi_i, \tilde{g}_{\mu\nu}A(\varphi)^2], \tag{4}$$

where the scalar-field potential $V(\varphi)$ takes the form [30,46]

$$V(\varphi) = \frac{(p-1)^2}{4ap^2} = \frac{(1 - exp(-2\varphi/\sqrt{3}))^2}{4a}. \tag{5}$$

By varying with respect to the metric $\tilde{g}_{\mu\nu}$ and the scalar field φ, one obtains the modified field equation in the Einstein frame

$$\tilde{G}_{\mu\nu} = 8\pi G[\tilde{T}_{\mu\nu} + T^{\varphi}_{\mu\nu}], \tag{6}$$

$$\nabla_\mu\nabla^\mu\varphi - \frac{1}{4}V_{,\varphi} = -4\pi G\alpha(\varphi)\tilde{T}, \tag{7}$$

where $T^{\varphi}_{\mu\nu}$ and $V_{,\varphi} \equiv \frac{dV(\phi)}{d\phi}$ where $T^{\varphi}_{\mu\nu}$ is the energy-momentum tensor corresponding to the scalar field and $V_{,\varphi} \equiv \frac{dV(\phi)}{d\phi}$. Furthermore, the coupling constant $\alpha(\varphi)$ exhibits a relationship with [7,47]

$$\alpha(\varphi) = \frac{d\ln A(\varphi)}{d\varphi} = -\frac{1}{\sqrt{3}}. \tag{8}$$

To that end, the energy-momentum tensor of the Einstein frame, denoted as $\tilde{T}_{\mu\nu}$, is connected to that of the Jordan frame, denoted as $T_{\mu\nu}$, by the equation $\tilde{T}_{\mu\nu} = A(\phi)^2T_{\mu\nu}$. Here, we assume that the matter content of the star is described by an isotropic fluid, which is characterized by

$$T^{\nu}_{i} = (\rho + P)u^\nu u_i + Pg^{\nu}_{i}, \tag{9}$$

where ρ is the energy density, P is the pressure, and u^ν is the four-velocity of the fluid, respectively. Using these, the energy-momentum tensor yields only the nonzero diagonal components as follows: $T_i^\nu = (-\rho, P, P, P)$. The energy density and pressure of the isotropic fluid are connected to the Einstein frame via [7,47] $\tilde{\epsilon} = A(\phi)^4\rho$ and $\tilde{P}_\perp = A(\phi)^4 P_\perp$, where the tilde indicates the Einstein frame.

In our analysis of non-rotating stars, we thus choose a spherically symmetric metric characterized by two unknowns, for which the line element is given by

$$ds^2 = -e^{2\Phi(r)}dt^2 + e^{2\Lambda(r)}dr^2 + r^2 d\Omega^2, \tag{10}$$

where $d\Omega^2 = d\theta^2 + \sin^2\theta d\vartheta^2$ is the line element on the unit 2-sphere, along with the metric functions $\Phi(r)$ and $\Lambda(r)$ that depend solely on the radial coordinate r.

Based on the above assumptions, we obtain the modified TOV equations in the nonperturbative method as follows (a detailed derivation is given in Refs. [7,47]:

$$\frac{1}{r^2}\frac{d}{dr}\left[r(1-e^{-2\Lambda})\right] = 8\pi A^4(\varphi)\rho + e^{-2\Lambda}\left(\frac{d\varphi}{dr}\right)^2 + \frac{1}{2}V(\varphi), \tag{11}$$

$$\frac{2}{r}e^{-2\Lambda}\frac{d\Phi}{dr} - \frac{1}{r^2}(1-e^{-2\Lambda}) = 8\pi A^4(\varphi)P + e^{-2\Lambda}\left(\frac{d\varphi}{dr}\right)^2 - \frac{1}{2}V(\varphi), \tag{12}$$

$$\frac{d^2\varphi}{dr^2} + \left(\frac{d\Phi}{dr} - \frac{d\Lambda}{dr} + \frac{2}{r}\right)\frac{d\varphi}{dr} = 4\pi\alpha(\varphi)A^4(\varphi)(\rho - 3P)e^{2\Lambda} + \frac{1}{4}\frac{dV(\varphi)}{d\varphi}e^{2\Lambda}, \tag{13}$$

$$\frac{dP}{dr} = -(\rho + P)\left(\frac{d\Phi}{dr} + \alpha(\varphi)\frac{d\varphi}{dr}\right). \tag{14}$$

The above set of Eqs. (11)–(14) describes the interior structure of dark energy stars. The modified TOV equations can be figured out when supplemented with an EoS $P = P(\rho)$, which we discuss later.

Here, we seek to determine the specific boundary conditions for Eqs. (11)–(14) to solve the interior and the exterior spacetime simultaneously. Thus, we require boundary conditions in the natural Einstein frame to ensure regularity at the origin,

$$\rho(0) = \rho_c, \quad \Lambda(0) = 0, \quad \varphi(0) = \varphi_c, \quad \frac{d\varphi}{dr}(0) = 0, \tag{15}$$

where ρ_c and ϕ_c denote the central value of energy density and the scalar field, respectively, while at infinity

$$\lim_{r\to\infty}\Phi(r) = 0, \quad \lim_{r\to\infty}\varphi(r) = 0. \tag{16}$$

The star's radius is identified using the condition

$$P(r_S) = 0, \tag{17}$$

i.e., the pressure vanishes at the surface of the star. As noted in [47], the condition $\frac{d\varphi}{dr}(0) = 0$ ensures the regularity of the scalar field ϕ, and consequently secures the regularity of Φ at the center of the star where $r = 0$. Ensuring the regularity of the Einstein frame geometry at the center requires $\Lambda(0) = 0$. Given that the Jordan and Einstein frame metrics are conformally related through a nonsingular conformal factor, this condition also ensures the regularity of the Jordan frame geometry at the star's center. In contrast, the boundary conditions are chosen to satisfy the asymptotic flatness requirement at infinity, which requires $\lim_{r\to\infty} V(\varphi(r)) = 0$, and leads to $\lim_{r\to\infty}\varphi(r) = 0$. The conditions specified in (16) ensure the asymptotic flatness in both the Einstein and Jordan frames.

Since the coordinate radius of the star is determined through Eq. (17), the physical radius of the star, as observed in the physical Jordan frame, is provided by

$$R_S = A[\varphi(r_S)]r_S. \tag{18}$$

3 Chaplygin model of dark energy

To obtain a complete description of the dark energy star, we consider the Chaplygin gas EoS, which has the potential to explain the unification of dark matter and dark energy [48–53]. It is worth pointing out that the Chaplygin scenario is phenomenologically consistent with the cosmic acceleration. This scenario is introduced by a more general Chaplygin-like EoS [54,55], that takes the following form [56]

$$P = A^2\rho - \frac{B^2}{\rho}. \tag{19}$$

where A (no unit) and B (units of energy density) are positive constants. Note that the pressure gradient approaches zero at the star's surface, and at this juncture, the energy density is $\rho_s = B/A$. Indeed, the causality condition ($v_s^2 = dP/d\rho < 1$) imposes limitations on the admissible values of the constant ($A^2 < 0.5$), see Refs. [14,16,17].

4 Numerical results and discussions

In this segment, we explore the structural properties of dark energy stars in hydrostatic equilibrium. Given the description of the modified Chaplygin equation of state (EoS) as specified in Eq. (19), we solve the modified TOV equations (11)–(14) for spherically symmetric, static stars, and subsequently generate mass–radius and mass–compactness curves. Our find-

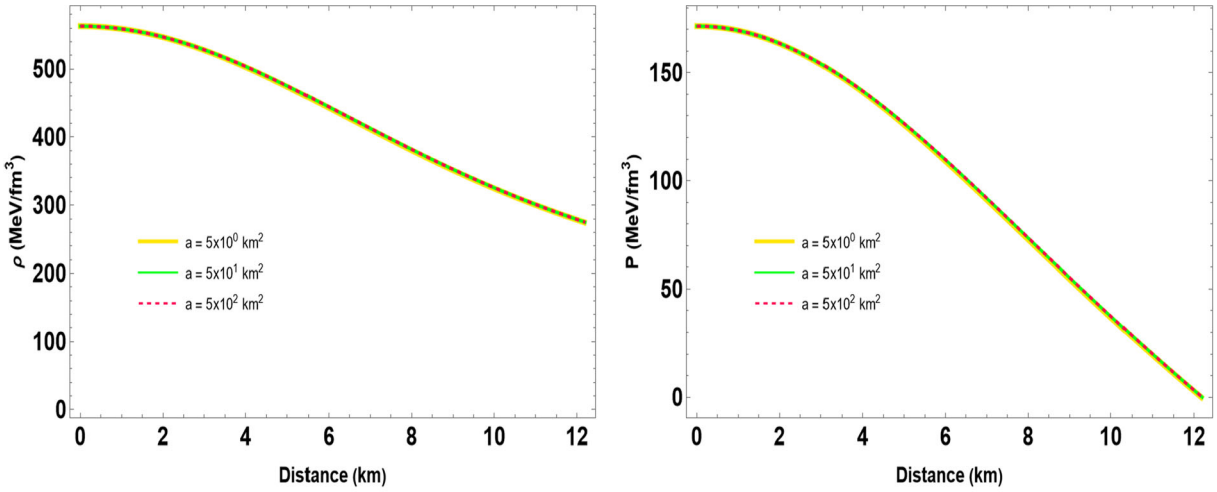

Fig. 1 **a** Energy density and **b** pressure as a function of radius for different values of $a \in [5, 50, 500]$ in km^2. The remaining parameters are fixed at $A^2 = 0.4$ and $B = 0.23 \times 10^{-3}$ km^{-2}

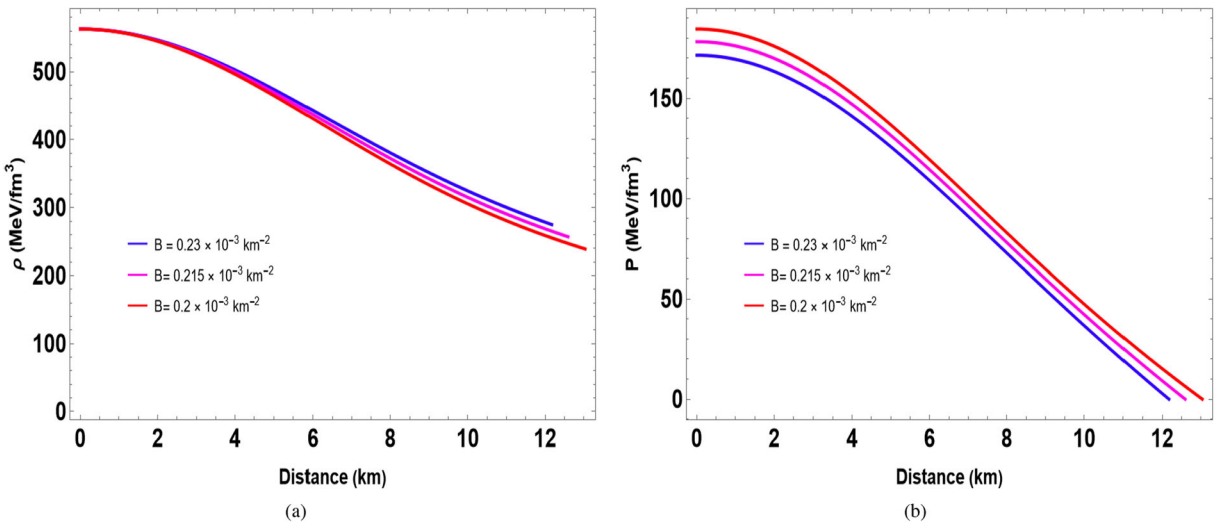

Fig. 2 (**a**) Energy density and (**b**) pressure as a function of radius for different values of $B \in [0.2, 0.215, 0.23] \times$ km^{-3} in km^{-2} The remaining parameters are fixed at $a = 5$ km^{-2} and $A^2 = 0.4$

Table 1 We present the main properties of our numerical findings concerning dark energy stars in variation of the R-squared gravity parameter a

a [km^2]	M [$M_\odot$]	R_M [km]	ρ_c [MeV/fm^3]	M/R
5×10^0	2.44	11.83	973	0.308
5×10^1	2.45	11.87	973	0.307
5×10^2	2.46	11.89	973	0.306

Table 2 We present the main properties of our numerical findings concerning dark energy stars in variation of the EoS parameter B within the framework of R-squared gravity

$B(\times 10^{-3})$ [km^{-2}]	M [$M_\odot$]	R_M [km]	ρ_c [MeV/fm^3]	M/R
0.200	2.64	12.71	973	0.307
0.215	2.54	12.28	872	0.306
0.230	2.46	11.83	973	0.308

ings are presented based on the variation of two parameter sets (a, B), which are listed in Tables 1 and 2, respectively. In all graphical representations, the maximum mass points are indicated by dots (Figs. 1, 2).

4.1 Profiles for variation of a

We first analyze the effect of the coupling constant a on the mass-radius ($M-R$) and mass-compactness ($M-M/R$) relations. In the case of R-squared gravity, we vary the parameter $a \in [5.0, 50, 500]$ in km^2, while maintaining the other parameters at $A^2 = 0.4$ and $B = 0.23 \times 10^{-3}$ km^{-2} as fixed. Our result for the given EoS of dark matter star is presented in Fig. 1a, b , depicting energy density and pressure as functions of radial distance. We can see that the density (pressure) attains its maximum value at the center of the star. As one moves toward the surface of the star, a decreasing trend is observed and ultimately reaching its minimum value at the surface. Next, we plot the ($M-R$) and ($M-M/R$) diagrams in Fig. 3a, b using the method described above. As shown in Fig. 3a , for larger a, the ($M-R$) curves are almost indistinguishable from each other. The observed trend in this study is comparable with the findings reported in our previous studies [62,63]. For clarity, we present the magnitude of the maximum masses and their corresponding radii in Table 1. For clarity, it is evident that the maximum mass exceeds $2M_\odot$, reaching up to 2.46 $M_\odot$ at $a = 500$ km^2. Finally, to verify the consistency of numerical calculations, we examine some of the constraints derived from astronomical and experimental observations. The upper horizontal band corresponds to the observational constraints from PSR J0952-0607, which has a mass of $M = 2.35 \pm 0.17 M_\odot$ (Magenta) [57]. Moreover, the highlighted mass and radius regions are based on the data extracted from NICER observations of the pulsars PSR J0030+0451 [59] and PSR J0740+6620 [58]. We also include gravitational wave observations constraints using the GW170817 event (blue contour regions) [60], while the estimated mass and radius of HESS J1731-347 [61] are illustrated within dark and light pink regions. By employing the above parametrization, we have computed the values of maximum compactness, as detailed in Table 1 for each respective case, and plotted the ($M-M/R$) curves in Fig. 3b . Turning then to the ($M-M/R$) sequences in Fig. 3b , we find that the curves are almost indistinguishable from one another, with the value reaching up to 0.306, as evident from Table 1. Furthermore, the table demonstrates that the Buchdahl limit is upheld, i.e., $M/R < 4/9$ [64].

4.2 Profiles for variation of B

Next, we turn our attention to the variation of the EoS parameter $B \in [0.23, 0.215, 0.2] \times 10^{-3}$ km^{-2}, while maintaining the other parameters, $a = 5$km^2 and $A^2 = 0.4$, as constants. In Figs. 2a, b , we display the energy density and pressure as functions of radial distance. These plots show a decreasing trend towards the star's surface, with the maximum values occurring at the center. Further, we have tested the sensitivity of our results in ($M-R$) and ($M-M/R$) relations. In Fig. 4a , we discuss the changes of the ($M-R$) relations obtained from the EoS (19) together with the predicted masses and radii of the pulsars PSR J0952-0607 [57], PSR J0030+0451 [59] and PSR J0740+6620 [58]. Additionally, we find that the ($M-R$) curve satisfies the constraints from the GW170817 event [60], as well as the low-mass ultracompact star HESS J1731-347 [61]. The mass constraint from the GW190425 event [65] is represented by the green horizontal band. Considering the choice of parameter B, we see that the maximum mass (corresponding radii) of dark-energy stars decreases with increasing values of B. The highest recorded mass is $M_{\max} = 2.64 M_\odot$, occurring at $B = 0.2 \times 10^{-3}$ km^{-2}. The obtained maximum mass is consistent with the GW190814 event. Subsequently, we plot the ($M-M/R$) relations in Fig. 4b . We observe that the M/R curves exhibit minimal variation in the low-mass region, whereas the deviation is more pronounced in the higher-mass region. The numerical values representing maximum compactness are presented in Table 2, which provides clear evidence that the Buchdahl limit is upheld, i.e., $M/R < 4/9$.

5 Criterion for static stability, the adiabatic index, and the speed of sound

Following our discussion on the proposed model's astrophysical feasibility, we plan to investigate the stability of dark energy stars using the static stability criterion, the adiabatic index, and the sound speed. Each of these aspects will be assessed sequentially and accompanied by visual representations.

5.1 Static stability criterion

Analyzing radial oscillation modes offers a promising approach for evaluating the stability of compact stars. This study emphasizes the *static stability criterion* [66,67], by plotting the total mass against central density, i.e., M vs. ρ_c, for dark energy stars. However, this condition is necessary for stability. It is not sufficient. We write the following inequalities:

$$\frac{dM}{d\rho_c} < 0 \quad \rightarrow \text{indicating an unstable configuration,} \tag{20}$$

$$\frac{dM}{d\rho_c} > 0 \quad \rightarrow \text{indicating a stable configuration.} \tag{21}$$

Our results for $M-\rho_c$ curves are shown in Fig. 5. In fact, for a stable configuration, the criterion $dM/d\rho_c > 0$ must

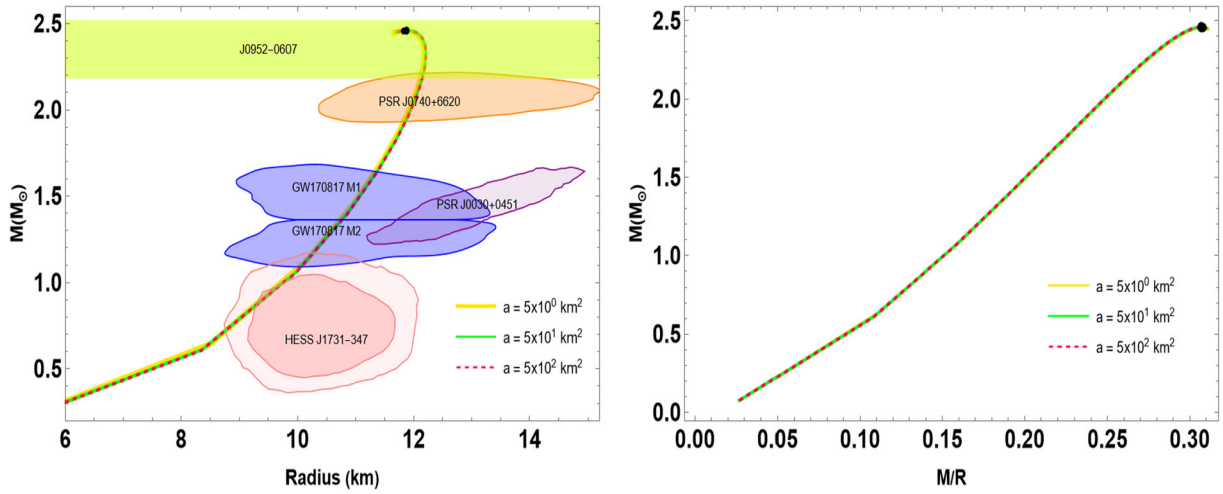

Fig. 3 **a** Mass-radius diagram with constraints derived from astronomical observations and **b** stellar mass as a function of compactness for a dark energy star, with variations in the R-squared gravity parameter a. The horizontal bands above 2 $M_\odot$ correspond to the observational constraints from PSR J0952-0607 (pastel green) [57]. The shaded areas correspond to the mass and radius measurements of NICER observations PSR J0740+6620 (orange) [58] and PSR J0030+0451 (pastel pink) [59], respectively. We have also included the GW170817 event (blue elliptic regions) [60], along with the low mass compact star HESS J1731-347 [61] (dark and light pink regions). Table 1 lists the parameters used in this analysis

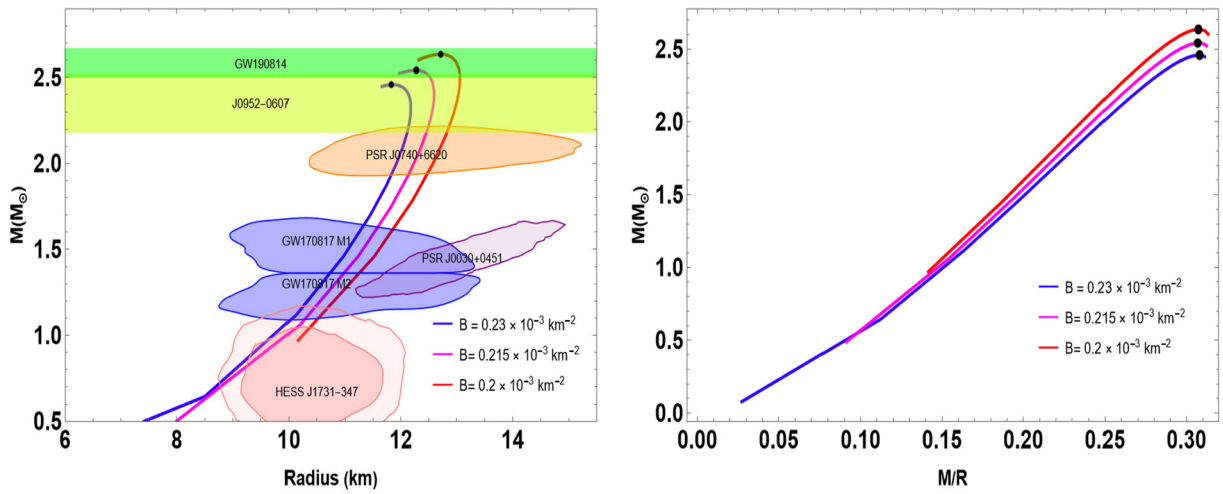

Fig. 4 **a** Mass-radius diagram with constraints derived from astronomical observations and **b** stellar mass as a function of compactness for a dark energy star, showing changes in the EoS parameter B within the framework of R-squared gravity. The shaded areas and horizontal bands with different colors correspond to different prior choices for NS mass and radius constraints, as depicted in Fig. 3a. The parameters used in this analysis are listed in Table 2

be satisfied. The star becomes unstable beyond this critical value (marked by a black circle).

5.2 Adiabatic indices

We now examine the behavior of the adiabatic index, γ, to assess the stability of astrophysical models. The dynamical stability of an equilibrium configuration was initially formulated by Chandrasekhar [68] in Einstein gravity. Later, this concept is applied to various modified gravity theories, including R-squared gravity, see Refs. [63,69] for more. To address this, we define the adiabatic index, γ, as follows:

$$\gamma \equiv \left(1 + \frac{\rho}{P}\right) v_s^2, \tag{22}$$

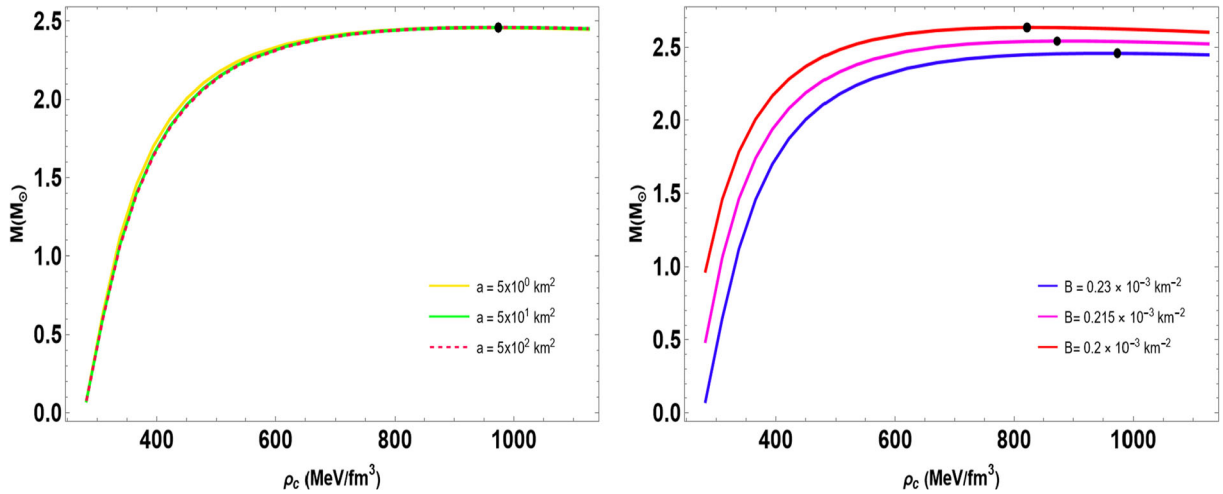

Fig. 5 The profiles of the mass versus central density relationships are examined using the same parameter sets as those presented in Tables 1 and 2

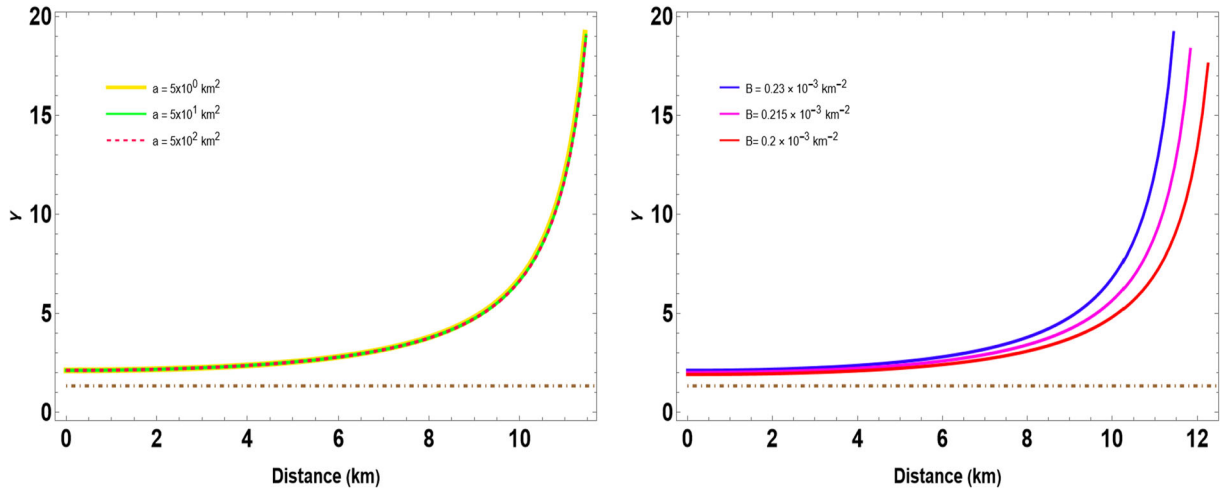

Fig. 6 The adiabatic index (γ) has been plotted against the radial coordinate r using the same parameter sets as those in Tables 1 and 2

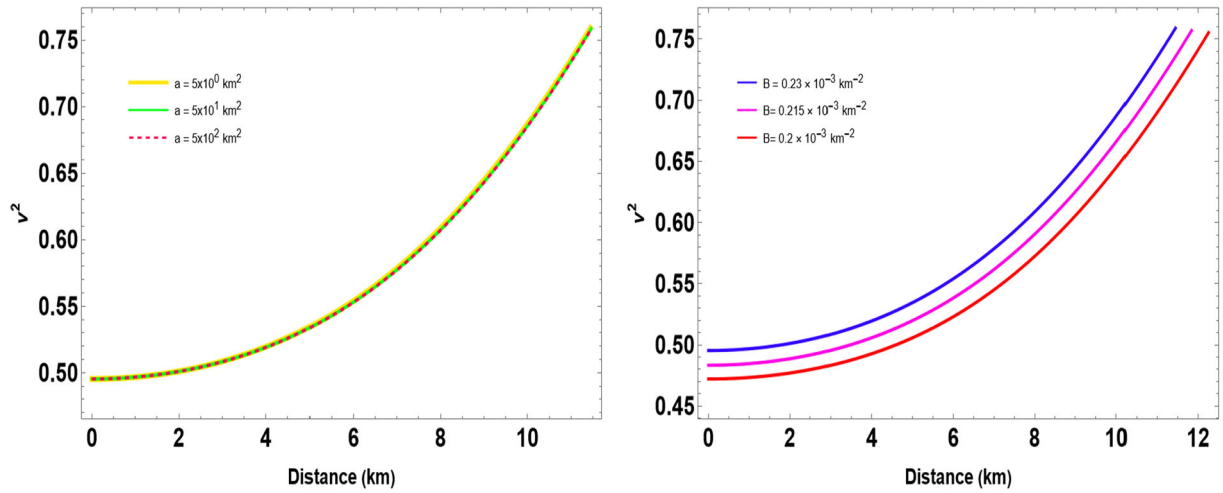

Fig. 7 The squared sound speed of dark matter stars computed using the same parameter sets as shown in Tables 1 and 2

where v_s^2 represents the speed of sound (in units of the speed of light). Strictly speaking, the value of γ, linked to the dynamical instability of an isotropic fluid sphere, has specific limitations. These limitations are referred to as the critical adiabatic index γ_{cr}, defined by the inequality $< \gamma >> \gamma_{cr}$, where $< \gamma >$ stands for the averaged adiabatic index [70]. Previous studies [70,71] have determined that the value of γ_{cr} is given by $\gamma_{cr} = \frac{4}{3} + \frac{19}{42}C$, where $C = 2\,M/R$ is the compactness parameter in GR. In Newtonian gravity, this value is $\gamma_{cr} = 4/3$; however, when the effects of GR are taken into account, this value exceeds 4/3 for the dynamical stability of an isotropic fluid sphere. By utilizing the field equations and Eqs. (19), we plot γ as a function of r in Fig. 6 for several representative values of (a, B) as detailed in Tables 1 and 2. The results show strong consistency with a configuration that is dynamically stable.

5.3 Sound speed and causality

In the following, we explore the behavior of sound speed, defined as $v^2 = \frac{dP}{d\rho}$, which must be lower than that of light, as indicated by the condition $v^2 < 1$. In Fig. 7, we show the behavior of the velocity of sound as a function of distance r. The figures confirm that both causality and stability conditions are met.

6 Summary and conclusions

In this study, we have conducted a comprehensive analysis of the structure and stability of dark energy stars under the $f(R)$ approach to gravity, within the framework of the Starobinsky model characterized by the Lagrangian $f(R) = R + aR^2$. The driving motivation behind this investigation has been to pursue singularity-free, stable alternatives to classical black holes in high-energy astrophysics and theories of gravity with quantum corrections. In doing so, we have treated the matter content using a modified Chaplygin gas EoS, as it provides a valid description for unifying both dark matter and dark energy behavior under a single fluid description.

Assuming spherical symmetry and isotropy, we derived the modified Tolman–Oppenheimer–Volkoff (TOV) equations, which were then solved numerically with appropriate boundary conditions. In our analysis, we examined the role of the R^2 gravity parameter a and the EoS parameter B on the structural properties of dark stars, namely energy density and pressure profiles, mass-radius $(M - R)$ relations, and compactness (M/R).

Key findings of this work can be summarized as follows:

- Our results show that changing the Starobinsky parameter a leads to modest shifts in the mass-radius relationship. For values $a \in [5, 50, 500]$ km^2, the maximum mass reaches up to $2.46M_\odot$, indicating that dark energy stars in this model comfortably satisfy current astrophysical constraints from massive pulsars, such as PSR J0952-0607 and PSR J0740+6620.
- On the other hand, the EoS parameter B has a more pronounced effect on stellar properties. Smaller values of B lead to increased maximum mass and radius, with $M_{\max} = 2.64M_\odot$ attained at $B = 0.2 \times 10^{-3}$ km^{-2}.
- The obtained solutions satisfy the Buchdahl bound $M/R < 4/9$, indicating physical viability.
- Stability analysis based on the static stability criterion $(dM/d\rho_c > 0)$, the adiabatic index γ, and the sound speed condition $v_s^2 < 1$, all affirm that the resulting configurations are stable against small perturbations and maintain causality throughout the star's interior.
- Theoretical predictions were benchmarked against observational data from NICER, LIGO/Virgo events (e.g., GW170817, GW190814), and low-mass compact stars such as HESS J1731-347. Our model is shown to be in strong agreement with these multi-messenger constraints.

These findings support the view that combining R^2 gravity with a modified Chaplygin gas equation of state leads to stable, regular, and physically realistic dark energy star models. The fact that these models predict higher maximum masses than those allowed by standard general relativity suggests they could help bridge the gap between theory and the large masses observed in some compact stars.

In future work, we plan to expand this framework by incorporating effects such as pressure anisotropy, rotation, and more advanced equations of state (EoS), particularly those derived from nuclear many-body theory or quantum chromodynamics (QCD). These extensions aim to deepen our understanding of the internal dynamics of exotic compact objects and the observational signals they may produce. Ultimately, this could provide new ways to distinguish them from traditional neutron stars and black holes in forthcoming gravitational wave and X-ray observations.

Acknowledgements J.R. acknowledges Grant No. F-FA-2021-510 of the Ministry of Higher Education, Science, and Innovations of the Republic of Uzbekistan. J.R. acknowledges the University of Hradec Kralove for hospitality and thanks to Excellence Project PřF UHK 2205/2025-2026.

Funding This work was supported by the Deanship of Scientific Research, Vice Presidency for Graduate Studies and Scientific Research, King Faisal University, Saudi Arabia (KFU252631).

Data Availability Statement This manuscript has no associated data. [Authors' comment: Data sharing does not apply to this paper, as no datasets were generated or analyzed during this study.]

Code Availability Statement This manuscript has no associated code/software. [Authors' comment: Code/Software sharing does not apply to this paper, as no code/software was generated or analyzed during the current study.]

Funded by SCOAP[3].

References

1. G. Chapline, Int. J. Mod. Phys. A **18**, 3587 (2003). https://doi.org/10.1142/S0217751X03016380
2. G. Chapline, eConf **0205**, C041213 (2004). arXiv:astro-ph/0503200
3. P.O. Mazur, E. Mottola, Universe **9**, 88 (2023). https://doi.org/10.3390/universe9020088. arXiv:gr-qc/0109035
4. S.S. Yazadjiev, D.D. Doneva, K.D. Kokkotas, Phys. Rev. D **91**, 084018 (2015). https://doi.org/10.1103/PhysRevD.91.084018. arXiv:1501.04591 [gr-qc]
5. R. Chan, M.F.A. da Silva, J.F. Villas da Rocha, Mod. Phys. Lett. A **24**, 1137 (2009). https://doi.org/10.1142/S0217732309028692. arXiv:0803.2508 [gr-qc]
6. F.S.N. Lobo, Class. Quantum Gravity **23**, 1525 (2006). https://doi.org/10.1088/0264-9381/23/5/006. arXiv:gr-qc/0508115
7. S.S. Yazadjiev, D.D. Doneva, K.D. Kokkotas, K.V. Staykov, JCAP **06**, 003 (2014). https://doi.org/10.1088/1475-7516/2014/06/003. arXiv:1402.4469 [gr-qc]
8. C.R. Ghezzi, Astrophys. Space Sci. **333**, 437 (2011). https://doi.org/10.1007/s10509-011-0663-4. arXiv:0908.0779 [gr-qc]
9. S.S. Yazadjiev, Phys. Rev. D **83**, 127501 (2011). https://doi.org/10.1103/PhysRevD.83.127501. arXiv:1104.1865 [gr-qc]
10. F. Rahaman, R. Maulick, A.K. Yadav, S. Ray, R. Sharma, Gen. Relativ. Gravit. **44**, 107 (2012). https://doi.org/10.1007/s10714-011-1262-y. arXiv:1102.1382 [gr-qc]
11. P. Beltracchi, P. Gondolo, Phys. Rev. D **99**, 044037 (2019). https://doi.org/10.1103/PhysRevD.99.044037. arXiv:1810.12400 [gr-qc]
12. M.F.A.R. Sakti, A. Sulaksono, Phys. Rev. D **103**, 084042 (2021). https://doi.org/10.1103/PhysRevD.103.084042. arXiv:2103.15393 [gr-qc]
13. G. Abellán, A. Rincon, E. Sanchez, Universe **9**, 352 (2023). https://doi.org/10.3390/universe9080352. arXiv:2308.12236 [gr-qc]
14. G. Panotopoulos, A. Rincón, I. Lopes, Eur. Phys. J. Plus **135**, 856 (2020). https://doi.org/10.1140/epjp/s13360-020-00867-x. arXiv:2010.09373 [gr-qc]
15. M.E. Akramov, J.R. Yusupov, M. Ehrhardt, H. Susanto, D.U. Matrasulov, **100**, 045209 (2025). https://doi.org/10.1088/1402-4896/adb914. arXiv:2408.03709 [math-ph]
16. G. Panotopoulos, A. Rincón, I. Lopes, Phys. Dark Univ. **34**, 100885 (2021). https://doi.org/10.1016/j.dark.2021.100885. arXiv:2109.05619 [gr-qc]
17. J.M.Z. Pretel, Eur. Phys. J. C **83**, 26 (2023). https://doi.org/10.1140/epjc/s10052-023-11198-3. arXiv:2301.03504 [gr-qc]
18. J.M.Z. Pretel, M. Dutra, S.B. Duarte, Phys. Rev. D **109**, 023524 (2024). https://doi.org/10.1103/PhysRevD.109.023524. arXiv:2401.01961 [astro-ph.HE]
19. O.P. Jyothilakshmi, L.J. Naik, V. Sreekanth, Eur. Phys. J. C **84**, 427 (2024). https://doi.org/10.1140/epjc/s10052-024-12776-9. arXiv:2403.00711 [gr-qc]
20. E. Berti, F. White, A. Maniopoulou, M. Bruni, Mon. Not. Roy. Astron. Soc. **358**, 923 (2005). https://doi.org/10.1111/j.1365-2966.2005.08812.x. arXiv:gr-qc/0405146
21. P. Bueno, P.A. Cano, F. Goelen, T. Hertog, B. Vercnocke, Phys. Rev. D **97**, 024040 (2018). https://doi.org/10.1103/PhysRevD.97.024040. arXiv:1711.00391 [gr-qc]
22. E.J. Copeland, M. Sami, S. Tsujikawa, Int. J. Mod. Phys. D **15**, 1753 (2006). https://doi.org/10.1142/S021827180600942X. arXiv:hep-th/0603057
23. K. Bamba, S. Capozziello, S. Nojiri, S.D. Odintsov, Astrophys. Space Sci. **342**, 155 (2012). https://doi.org/10.1007/s10509-012-1181-8. arXiv:1205.3421 [gr-qc]
24. S.K. Maurya, F. Tello-Ortiz, Phys. Dark Univ. **27**, 100442 (2020). https://doi.org/10.1016/j.dark.2019.100442. arXiv:1905.13519 [gr-qc]
25. A. Paliathanasis, M. Tsamparlis, S. Basilakos, J.D. Barrow, Phys. Rev. D **93**, 043528 (2016). https://doi.org/10.1103/PhysRevD.93.043528. arXiv:1511.00439 [gr-qc]
26. M. Malaver, H.D. Kasmaei, R. Iyer, S. Sadhukhan, A. Kar, (2021). arXiv:2106.09520 [gr-qc]
27. M.M. Suleimanov, M.U. Nosirov, H.T. Yusupov, A. Chaves, G.R. Berdiyorov, K.Y. Rakhimov, arXiv e-prints (2024). https://doi.org/10.48550/arXiv.2411.02896. arXiv:2411.02896 [cond-mat.mes-hall]
28. M. Sharif, A. Waseem, PTEP **2019**(5), 053E02 (2019). https://doi.org/10.1093/ptep/ptz041. arXiv:1904.05885 [gr-qc]
29. A. De Felice, S. Tsujikawa, Living Rev. Relativ. **13**, 3 (2010). https://doi.org/10.12942/lrr-2010-3. arXiv:1002.4928 [gr-qc]
30. P. Brax, C. van de Bruck, A.-C. Davis, D.J. Shaw, Phys. Rev. D **78**, 104021 (2008). https://doi.org/10.1103/PhysRevD.78.104021. arXiv:0806.3415 [astro-ph]
31. M.K. Mak, T. Harko, Eur. Phys. J. C **73**, 2585 (2013). https://doi.org/10.1140/epjc/s10052-013-2585-5. arXiv:1309.5123 [gr-qc]
32. A. Bagheri Tudeshki, G.H. Bordbar, B. Eslam Panah, Phys. Lett. B **848**, 138333 (2024). https://doi.org/10.1016/j.physletb.2023.138333. arXiv:2311.13138 [gr-qc]
33. M. Kumar, J. Kumar, Phys. Scr. **98**, 035012 (2023). https://doi.org/10.1088/1402-4896/acb8ef
34. R.C. Tolman, Phys. Rev. **55**, 364 (1939). https://doi.org/10.1103/PhysRev.55.364
35. A. Borowiec, A. Stachowski, M. Szydłowski, A. Wojnar, J. Cosmol. Astropart. Phys. **2016**(01), 040 (2016). https://doi.org/10.1088/1475-7516/2016/01/040
36. K. Karami, M.S. Khaledian, M.S. Khaledian, Int. J. Mod. Phys. D **21**, 1250083 (2012). https://doi.org/10.1142/S0218271812500836. arXiv:1010.2639 [physics.gen-ph]
37. M. Zubair, G. Abbas, Study of anisotropic compact stars in Starobinsky model. (2016). arXiv:1412.2120 [physics.gen-ph]
38. A. Errehymy, M. Daoud, Found. Phys. **49**, 144 (2019). https://doi.org/10.1007/s10701-019-00237-3
39. A. Malik, T. Naz, F. Mofarreh, A. Shazadi, Int. J. Geom. Methods Mod. Phys. **21**, 2450086 (2024). https://doi.org/10.1142/S0219887824500865
40. M. Elmardi, A. Abebe, A. Tekola, Int. J. Geom. Methods Mod. Phys. **13**, 1650120 (2016). https://doi.org/10.1142/S0219887816501206. arXiv:1603.05535 [gr-qc]
41. B. Turimov, S. Usanov, Y. Khamroev, Phys. Dark Univ. **48**, 101876 (2025). https://doi.org/10.1016/j.dark.2025.101876. arXiv:2502.11185 [gr-qc]

42. H.R. Fazlollahi, Phys. Lett. B **781**, 542 (2018). https://doi.org/10.1016/j.physletb.2018.04.031. arXiv:1804.02971 [gr-qc]
43. A. Stachowski, M. Szydłowski, A. Borowiec, Eur. Phys. J. C **77**, 406 (2017). https://doi.org/10.1140/epjc/s10052-017-4981-8. arXiv:1608.03196 [gr-qc]
44. T.P. Sotiriou, V. Faraoni, Rev. Mod. Phys. **82**, 451 (2010). https://doi.org/10.1103/RevModPhys.82.451. arXiv:0805.1726 [gr-qc]
45. A.S. Arapoglu, C. Deliduman, K.Y. Eksi, JCAP **07**, 020 (2011). https://doi.org/10.1088/1475-7516/2011/07/020. arXiv:1003.3179 [gr-qc]
46. R.P. Woodard, Lect. Notes Phys. **720**, 403 (2007). arXiv:astro-ph/0601672
47. K.V. Staykov, D.D. Doneva, S.S. Yazadjiev, K.D. Kokkotas, JCAP **10**, 006 (2014). https://doi.org/10.1088/1475-7516/2014/10/006. arXiv:1407.2180 [gr-qc]
48. A.Y. Kamenshchik, U. Moschella, V. Pasquier, Phys. Lett. B **511**, 265 (2001). https://doi.org/10.1016/S0370-2693(01)00571-8. arXiv:gr-qc/0103004
49. N. Bilic, G.B. Tupper, R.D. Viollier, Phys. Lett. B **535**, 17 (2002). https://doi.org/10.1016/S0370-2693(02)01716-1. arXiv:astro-ph/0111325
50. M.C. Bento, O. Bertolami, A.A. Sen, Phys. Rev. D **66**, 043507 (2002). https://doi.org/10.1103/PhysRevD.66.043507. arXiv:gr-qc/0202064
51. V. Gorini, A. Kamenshchik, U. Moschella, Phys. Rev. D **67**, 063509 (2003). https://doi.org/10.1103/PhysRevD.67.063509. arXiv:astro-ph/0209395
52. X. Zhang, F.-Q. Wu, J. Zhang, JCAP **01**, 003 (2006). https://doi.org/10.1088/1475-7516/2006/01/003. arXiv:astro-ph/0411221
53. L. Xu, J. Lu, Y. Wang, Eur. Phys. J. C (2012). https://doi.org/10.1140/epjc/s10052-012-1883-7
54. B. Pourhassan, Int. J. Mod. Phys. D **22**, 1350061 (2013). https://doi.org/10.1142/S0218271813500612. arXiv:1301.2788 [gr-qc]
55. H. Saadat, B. Pourhassan, Astrophys. Space Sci. **344**, 237 (2013). https://doi.org/10.1007/s10509-012-1301-5
56. E.O. Kahya, B. Pourhassan, Mod. Phys. Lett. A **30**, 1550070 (2015). https://doi.org/10.1142/S0217732315500704. arXiv:1502.01189 [gr-qc]
57. R.W. Romani, D. Kandel, A.V. Filippenko, T.G. Brink, W. Zheng, Astrophys. J. Lett. **934**, L17 (2022). https://doi.org/10.3847/2041-8213/ac8007. arXiv:2207.05124 [astro-ph.HE]
58. M.C. Miller et al., Astrophys. J. Lett. **918**, L28 (2021). https://doi.org/10.3847/2041-8213/ac089b. arXiv:2105.06979 [astro-ph.HE]
59. T.E. Riley et al., Astrophys. J. Lett. **887**, L21 (2019). https://doi.org/10.3847/2041-8213/ab481c. arXiv:1912.05702 [astro-ph.HE]
60. B.P. Abbott et al. (LIGO Scientific, Virgo), Phys. Rev. Lett. **121**, 161101 (2018). https://doi.org/10.1103/PhysRevLett.121.161101. arXiv:1805.11581 [gr-qc]
61. V. Doroshenko, V. Suleimanov, G. Pühlhofer, A. Santangelo, Nat. Astron. **6**, 1444 (2022). https://doi.org/10.1038/s41550-022-01800-1
62. G. Panotopoulos, T. Tangphati, A. Banerjee, M.K. Jasim, Phys. Lett. B **817**, 136330 (2021). https://doi.org/10.1016/j.physletb.2021.136330. arXiv:2104.00590 [gr-qc]
63. T. Tangphati, I. Sakallı, A. Banerjee, A. Pradhan, (2024). arXiv:2411.06170 [hep-th]
64. H.A. Buchdahl, Phys. Rev. **116**, 1027 (1959). https://doi.org/10.1103/PhysRev.116.1027
65. R. Abbott et al. (LIGO Scientific, Virgo), Astrophys. J. Lett. **896**, L44 (2020). https://doi.org/10.3847/2041-8213/ab960f. arXiv:2006.12611 [astro-ph.HE]
66. B.K. Harrison, K.S. Thorne, M. Wakano, J.A. Wheeler, *Gravitation Theory and Gravitational Collapse* (1965)
67. Y.B. Zeldovich, I.D. Novikov, *Relativistic Astrophysics. Vol.1: Stars and Relativity* (1971)
68. S. Chandrasekhar, Astrophys. J. **140**, 417 (1964). https://doi.org/10.1086/147938. [Erratum: Astrophys. J. 140, 1342 (1964)]
69. J.C. Jiménez, J.M.Z. Pretel, E.S. Fraga, S.E. Jorás, JCAP **07**(07), 017 (2022). https://doi.org/10.1088/1475-7516/2022/07/017. arXiv:2112.09950 [gr-qc]
70. C.C. Moustakidis, Gen. Relativ. Gravit. **49**, 68 (2017). https://doi.org/10.1007/s10714-017-2232-9. arXiv:1612.01726 [gr-qc]
71. P.S. Koliogiannis, C.C. Moustakidis, Astrophys. Space Sci. **364**, 52 (2019). https://doi.org/10.1007/s10509-019-3539-7. arXiv:1806.09999 [nucl-th]